

# Macrocyclic Peptides Closed by a Thioether–Bipyridyl Unit That Grants Cell Membrane Permeability

Hongxue Chen, Takayuki Katoh, and Hiroaki Suga\*

Cite This: *ACS Bio Med Chem Au* 2023, 3, 429–437

Read Online

ACCESS |



Metrics &amp; More



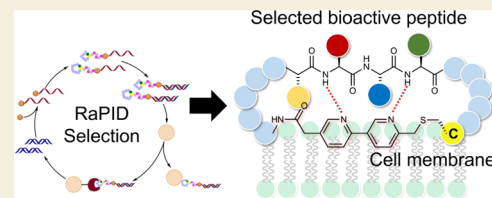
Article Recommendations



Supporting Information

**ABSTRACT:** Membrane permeability is an important factor that determines the virtue of peptides targeting intracellular molecules. By introducing a membrane penetration motif, some peptides exhibit better membrane permeabilities. Previous choices for such motifs have usually been polycationic sequences, but their protease vulnerabilities and modest endosome escapability remain challenging. Here, we report a strategy for macrocyclization of peptides closed by a hydrophobic bipyridyl (BPy) unit, which grants an improvement of their membrane permeability and proteolytic stability compared with the conventional polycationic peptides. We chemically prepared model macrocyclic peptides closed by a thioether–BPy unit and determined their cell membrane permeability, giving 200 nM CP<sub>50</sub> (an indicative value of membrane permeability), which is 40-fold better than that of the ordinary thioether macrocycle consisting of the same sequence composition. To discover potent target binders consisting of the BPy unit, we reprogrammed the initiator with chloromethyl–BPy (C<sup>Me</sup>BPy) for the peptide library synthesis with a downstream Cys residue(s) and executed RaPID (Random nonstandard Peptide Integrated Discovery) against the bromodomains of BRD4. One of the obtained sequences exhibited a single-digit nanomolar dissociation constant against BRD4 *in vitro* and showed approximately 2-fold and 10-fold better membrane permeability than positive controls, R9 and Tat peptides, respectively. Moreover, we observed an intracellular activity of the BPy macrocycle tagged with a proteasome target peptide motif (RRRG), resulting in modest but detectable degradation of BRD4. The present demonstration indicates that the combination of the RaPID system with an appropriate hydrophobic unit, such as BPy, would provide a potential approach for devising cell penetrating macrocycles targeting various intracellular proteins.

**KEYWORDS:** cyclic peptide, membrane permeability, cell penetrating peptides, mRNA display, *in vivo* protein degradation



## INTRODUCTION

A class of nontraditional peptides containing unique non-proteinogenic amino acids and a nonreducible macrocyclic scaffold has become an alternative modality to devise drug candidates with high affinity and specificity to target protein molecules.<sup>1,2</sup> Our group has worked on devising a platform technology to rapidly discover potent macrocyclic peptides, referred to as the RaPID (Random nonstandard Peptide Integrated Discovery) system, involving the combination of genetic code reprogramming facilitated by flexizymes and mRNA display.<sup>3–5</sup> By means of this system, we have identified various thioether-closed macrocycles consisting of proteinogenic and nonproteinogenic amino acids, such as *N*-methyl-L- $\alpha$ -amino acids, *D*- $\alpha$ -amino acids, and even  $\beta/\gamma$ -amino acids, having not only a strong binding ability to target proteins of interest but also potent biological activities.<sup>6,7</sup> Thus, it has been proven that the RaPID system is a robust and reliable platform for the discovery of novel peptidic drug candidates. Despite the potency of these macrocycles, finding those capable of penetrating cell membranes is yet a fortuitous event, and thereby only a limited number of macrocyclic peptides have exhibited intracellular activities.<sup>8–10</sup> Clearly, the membrane permeabilities of such macrocyclic peptides are largely

dependent on their three-dimensional structures and their dynamics, which are not yet readily predictable by simply looking at the primary sequence compositions.<sup>11–13</sup>

Polycationic peptides, such as Tat and poly-Arg (such as R9), are well known to make arbitrary peptides more membrane permeable. Such polycationic residues interact with the anionic membrane surface via electrostatic interactions and induce curvature formation on the membrane<sup>14</sup> (Figure 1a), which is captured by endocytosis-promoting factors.<sup>15</sup> However, this event could also result in cytotoxicity depending on the cell kind. More recently, Pei et al. prepared macrocyclic peptides embedding 3–5 residues of Arg in a combination of hydrophobic residues and elegantly demonstrated that such peptides were membrane permeable and exhibited inhibitory activity against intracellular target proteins with a varied range of activities.<sup>16–18</sup> A possible drawback of

Received: April 29, 2023

Revised: July 9, 2023

Accepted: July 10, 2023

Published: August 13, 2023



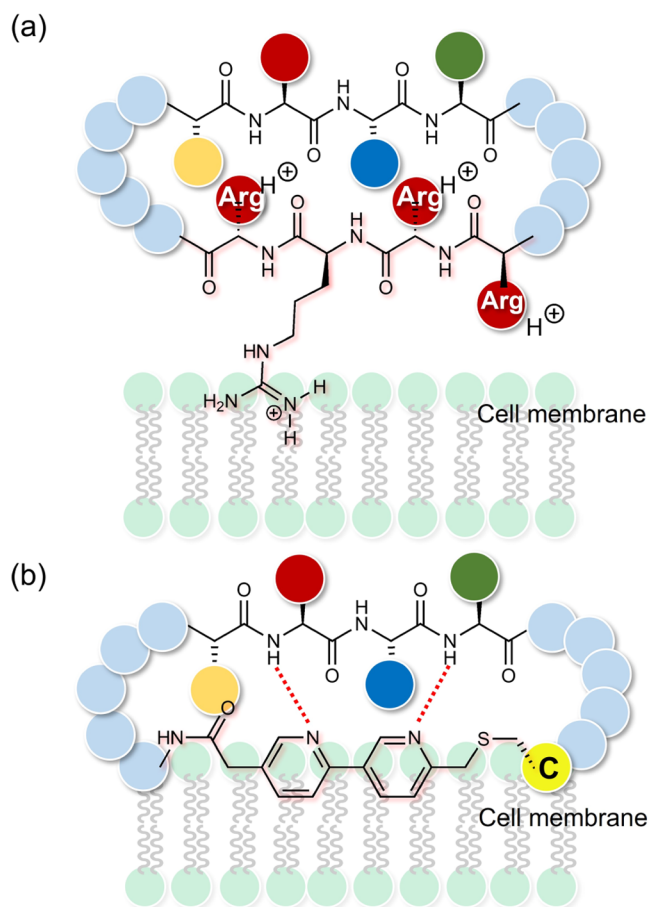


**Figure 1.** Schematic representation of two strategies among various others to enhance the cell membrane permeability of macrocyclic peptides. (a) Electrostatic interactions and hydrogen bonds between polycationic structures and membrane phospholipids could generate membrane curvature and promote cellular uptake. (b) Bipyridyl (BPy)–thioether unit of macrocyclic peptides examined in this work, which could enhance cell membrane permeability.

this approach is that the polycationic residues could constitute the recognition site for serum proteases, like trypsin,<sup>19</sup> and also require a similar mechanism of endocytosis for the release to the cytoplasm. Instead, it has been demonstrated that hydrophobic internal linkages, such as an alkyne/alkene staple or a biphenyl bond, were used to bridge or cyclize the peptides (Figure 1b).<sup>20–22</sup> This type of approach largely relies on the semirational design of  $\alpha$ -helical peptides,<sup>23</sup> yet such linkages enhance the overall hydrophobicity and successfully enhance the membrane permeability of the parental ones.<sup>24</sup> On the other hand, few examples are known in the literature for using such a hydrophobic linkage in non- $\alpha$ -helical peptides or applying it to a display approach to elaborate the cell membrane permeability of outputs.<sup>25,26</sup> Here, we report a ribosomal synthesis of macrocyclic peptides closed by a thioether–bipyridyl unit and performed the RAPID campaign to identify potent binders against a protein target, BRD4 (bromodomain-containing protein 4), as a model case. The bipyridyl (BPy) unit was designed to play two-fold roles, serving a hydrophobic unit and a hydrogen bond acceptor via the pyridine's nitrogen atom, to which NH groups in the opposite strand of the peptide coordinate. Such macrocycles have exhibited better membrane permeability than the ordinary thioether bond consisting of an acetyl unit and even

better than the polycationic peptides. We have also derived such peptides conjugated with a simple proteasome-targeting peptide motif, RRRG, via a polyethylene glycol linker, one of which could induce the degradation of BRD4 in cells.

## RESULTS

### Improvement of Membrane Permeabilities of Model Cyclic Peptides Closed by a Thioether–Bipyridyl Unit

We first designed and chemically synthesized a bipyridyl unit, 2-(6'-(chloromethyl)-[2,3'-bipyridine]-5-yl)acetic acid (<sup>ClMe</sup>BPy–COOH), for a macrocyclization building block. The synthesis of <sup>ClMe</sup>BPy–COOH was completed in 4 steps with an overall yield of 22% (Scheme S1). This molecule can be placed at the N-terminus of peptides, and its chloromethyl moiety allows nucleophilic substitution by a thiol group in a downstream cysteine (Cys, C) residue to cyclize the linear sequence via a thioether bond. In a similar manner, we also synthesized <sup>BrMe</sup>BPh–COOH as a control building block to evaluate the effectiveness of bipyridine over the biphenyl group (Scheme S2).

We then designed two model peptide sequences, **1** and **2**, consisting of (GS)<sub>6</sub>C and (RADA)<sub>3</sub>C, respectively.<sup>27,28</sup> Since both model peptides have no net charge, we expected that they would have little electrostatic interaction with the cell membrane, giving no major contribution to their passive membrane permeabilities. The N-terminus of each peptide had either <sup>ClMe</sup>BPy, bromomethyl biphenyl formic acid (<sup>BrMe</sup>BPh), or chloroacetyl tyrosine (<sup>ClAcY</sup>), allowing nucleophilic substitution by a thiol group in downstream Cys to cyclize the linear sequence via a thioether bond. We thus referred to these peptides as BPy1, BPy2, BPh1, BPh2, Y1, and Y2. The membrane permeabilities of these model peptides were determined by a chloroalkane penetration assay (CAPA). CAPA is a methodology developed by the Kritzer group for quantitatively evaluating the membrane permeability of a chloroalkane (CA)-tagged ligand molecule to cells that overexpress the HaloTag protein in cytosol<sup>29</sup> (Supporting Figure S1a). We synthesized the respective model peptides bearing the K<sup>\*</sup>-NH<sub>2</sub> sequence at the C-terminus, where the  $\epsilon$ -amino group of K<sup>\*</sup> was modified with a CA tag (BPy1-K<sup>\*</sup>, BPy2-K<sup>\*</sup>, BPh1-K<sup>\*</sup>, BPh2-K<sup>\*</sup>, Y1-K<sup>\*</sup>, and Y2-K<sup>\*</sup>; Figure 2a). Moreover, small-molecule positive and negative controls (CA-Trp and CA-Asp, respectively) and two peptide controls (CA-Antp and DPI-K<sup>\*</sup>) were tested for comparison in CAPA (see Supporting Figure S1b). Various concentrations of each peptide-K<sup>\*</sup> (10<sup>1</sup>–10<sup>5</sup> nM), as well as controls, were incubated with the cells (Figure 2b,c, as well as Supporting Figure S1c) for 4 h, in which those penetrating the cell membrane could be captured by the intracellular HaloTag proteins. The free HaloTag protein in the cells was traced by chloroalkane-tagged TAMRA (TAMRA-CA). The fluorescence intensity of captured TAMRA-CA in cells should reflect the membrane permeability of the respective peptide-K<sup>\*</sup> and control-CAs, represented by a CP<sub>50</sub> value, which refers to the concentration where half of peptide-CA was conjugated to the cellular HaloTag protein.

From the normalized fluorescence (0 for cells incubated with culture medium instead of TAMRA-CA and 100 for cells incubated with culture medium instead of peptide-CA) for various concentrations of model peptide-K<sup>\*</sup>s and control-CAs, sigmoidal fitting curves were generated, and their CP<sub>50</sub> values were calculated accordingly (Figure 2b,c). In model peptide **1**,

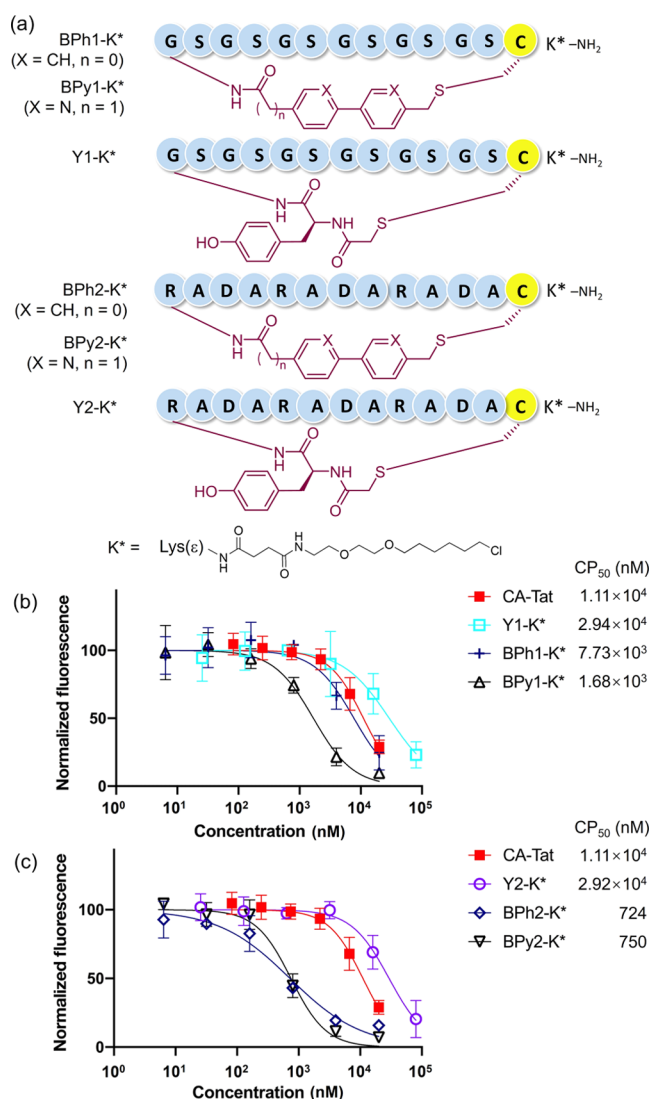


**Figure 2.** Model macrocyclic peptides closed by the biphenyl (BPh) and bipyridyl (BPy) thioether unit have greater membrane permeability than those closed by a standard acetyl-thioether unit. (a) Structures of model macrocyclic peptides bearing a chloroalkane tag (peptide-CA) studied in this work. (b, c) CAPA results of model peptide-CA molecules (4 h incubation). The fluorescence of TAMRA was normalized (0 for cells incubating with culture medium instead of TAMRA-CA and 100 for cells incubating with culture medium instead of peptide-CA). The introduction of the BPh or BPy thioether unit significantly lowered the CP<sub>50</sub> values of model peptides.

the CP<sub>50</sub> value of BPy1-K\* was one order of magnitude lower (*i.e.*, 10-fold better membrane permeability) than those of CA-Tat and Y1-K\* and approximately 5-fold lower than that of BPh1-K\*. This data suggests that the BPy linkage plays an enhancing role in the membrane permeability of the cyclic peptide. A similar trend was also observed for model peptide 2; BPy1-K\* has more than an order of magnitude higher membrane permeability than CA-Tat (13-fold) and Y2-K\* (40-fold). Interestingly, BPy2-K\* and BPh2-K\* have similar CP<sub>50</sub> values, suggesting that the effect of BPy vs. BPh on membrane permeability could depend on the peptide composition. Note that our other controls gave expected CP<sub>50</sub> values (Supporting Figure S1c), indicating that the difference in CP<sub>50</sub> values should be valid for the evaluation of membrane permeability. We also determined the CP<sub>50</sub> values

in 24 h incubation, showing that the observed values were smaller than those during 4 h, but the trend in comparison of the respective molecules remained the same (Supporting Figure S2). Nevertheless, the peptide model studies clearly indicate that the bipyridyl unit contributes to the enhancement of membrane permeabilities of the cyclic peptides.

### Construction of a BPy-Initiated Cyclic Peptide Library

Encouraged by the above results, we then sought to install the BPy unit in a library of macrocyclic peptides by means of the FIT (Flexible In vitro Translation) system. The library was then applied to the RaPID system. The initiator AUG codon was then reprogrammed to <sup>CLiMe</sup>BPy using tRNA<sub>CAU</sub><sup>fMet</sup> in a Met-deficient FIT system. We synthesized the cyanomethyl ester of <sup>CLiMe</sup>BPy (<sup>CLiMe</sup>BPy-CME) and tested for the flexizyme-assisted tRNA acylation (Scheme S1). Although the acylation product was undetected under the generic conditions on ice, elevating the reaction temperature to 25 °C and prolonged incubation time led the acylation product to a 21% yield (Figure S3).

By the use of <sup>CLiMe</sup>BPy-tRNA<sub>CAU</sub><sup>fMet</sup>, we translated a <sup>CLiMe</sup>BPy-initiated model peptide. Upon successful translation, the thiochloromethyl substitution would occur spontaneously to yield the thioether-BPy macrocyclic peptide. *m/z* corresponding to the desired cyclic peptide was found in the MALDI-TOF spectrum of the translated product, although a byproduct lacking BPy at the N-terminus derived from an N-terminal drop-off-reinitiation event<sup>30,31</sup> was also observed (Figure S4a). By increasing the concentration of <sup>CLiMe</sup>BPy-tRNA<sub>CAU</sub><sup>fMet</sup> to 100 μM, however, we were able to diminish the formation of the truncated peptide and express the desired peptide as the major product (Figure S4b). Then, the peptide library was constructed to have random peptide sequences encoded by an (NNK)<sub>10–15</sub> codon repeat and flanked by AUG <sup>CLiMe</sup>BPy and UGC Cys, followed by a (Gly-Ser)<sub>3</sub> linker peptide sequence as a spacer for the linkage of mRNA via puromycin (Figure S5a).

### RaPID Selection against BRD4

Bromodomain-containing protein 4 (BRD4, UniProt O60885) is a transcription coactivator overexpressed in various cancer cells, including myeloid leukemia cells,<sup>32</sup> prostate cancer cells,<sup>33</sup> and breast cancer cells.<sup>34</sup> Inhibition or degradation of BRD4 leads to suppression of the growth of these cancer cells and induction of their apoptosis, making BRD4 a potential epigenetic therapeutic target.<sup>35,36</sup> A small molecular antagonist targeting bromodomains, known as JQ-1, is an effective inhibitor of BRD4 with IC<sub>50</sub> of 28 nM,<sup>37</sup> and it has been used for the development of an effective PROTAC (proteolysis-targeting chimera) by conjugating with lenalidomide. Some peptidic ligands specific to BRD4 or its bromodomains have also been devised, but they are not membrane permeable, so neither the cellular antagonist nor PROTAC was developed.<sup>38,39</sup> This motivated us to devise membrane-permeable macrocycles targeting BRD4 as a showcase of this approach.

Following our standard selection protocol (Figure S5b), an mRNA encoding library of <sup>CLiMe</sup>BPy-initiated peptides was ligated to a 3'-puromycin-linked oligonucleotide to yield the thioether-BPy macrocycles-mRNA fusion library. The library was reverse transcribed and subsequently subjected to the “negative selection” against naked magnetic beads, followed by “positive selection” against His10-BRD4<sup>49–460</sup> (residues of 49–460, corresponding to bromodomains 1 and 2) immobilized on the same magnetic beads. The recovery rate of cDNA of the positive selection significantly increased in the 6th round, while

that of the negative selection stayed in the background level (Figure S5c). The enriched cDNA library after the 6th and 7th rounds was then sequenced, where a single species of the consensus sequence dominated in the enriched sequences (Figure S5d, the (GS)<sub>3</sub> linker was omitted and not included in the following experiments).

Since the sequences obtained from the selection contain two Cys residues (upstream Cys appeared in the random region), the respective isomers were chemically synthesized as follows. Both isomers with the C-terminal glycine carboxylamide were chemically synthesized with SPPS (solid-phase peptide synthesis) using orthogonally protected Cys residues and then cyclized after the intended Cys was selectively deprotected. The respective isomers were purified with HPLC to give a macrocyclic isomer (M1G) and a lariat isomer (L1G) (Figure 3a). Surface plasmon resonance (SPR) experiments showed

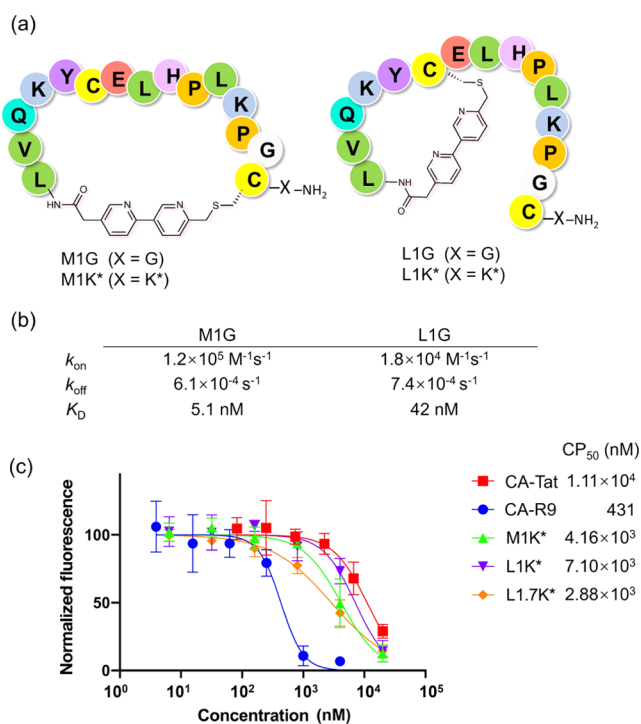


**Figure 3.** Macrocytic peptides closed by a bipyridyl thioether unit selected by the RaPID system against BRD4<sup>49–460</sup>. (a) Structures of two constitutional isomers of the selected peptide sequence referred to as M1 (macrocyclic) and L1 (lariat). (b) Kinetic values of M1G (G = Gly) and L1G binding with BRD4 determined by a surface plasmon resonance (SPR) method. The observed dissociation rate constants ( $k_{off}$ ) are nearly the same for both peptides, while a 10-fold higher association rate constant ( $k_{on}$ ) of M1G resulted in a lower  $K_D$  value than that of L1G. (c) CAPA results of the respective peptides. The observed  $CP_{50}$  values indicate that M1K\*, L1K\*, and L1.7K\* showed better than or comparable cell membrane permeabilities to CA-Tat, yet poorer than CA-R9.

that both isomers exhibited binding affinities to BRD4<sup>49–460</sup> in the nanomolar range (Figure S7), where M1G has a  $K_D$  of 5.1 nM and L1G has a  $K_D$  of 42 nM (Figure 3b). We then evaluated the stability of both peptide isomers in human serum at 37 °C (Figure S8). Both peptide isomers exhibited long half-lives (30 h for M1G and 26 h for L1G). On the other hand, the polycationic CPPs and Tat and R9 (both have the C-terminal carboxylamide) were rapidly degraded (their half-lives are 1.4 and 1.9 min, respectively).

### Selected Peptides are Membrane-Permeable Ligands of BRD4 Bromodomains

Next, we evaluated the membrane permeability of the peptides by means of CAPA. We also prepared a 7-residue macrocyclic structure of L1 [c(S-MeBPy-LVQKYC-)], referred to as L1.7, to see if the shorter peptide version acts better for membrane permeability. The chloroalkane-tagged peptides at the C-terminus (M1K\*, L1K\*, and L1.7K\*, as well as CA-Tat and CA-R9 as controls) were prepared and applied to CAPA following the same protocol described earlier. The normalized fluorescence and generated sigmoidal fitting curves are shown in Figure 3c with  $CP_{50}$  values. All three peptides exhibited  $CP_{50}$  values between CA-R9 and CA-Tat within 4 h. Notably, after incubating with cells for 24 h, these peptides exhibited comparable  $CP_{50}$  values in a range of 600 nM, which was 10-fold lower than that of CA-Tat (Figure S2b).

Finally, we explored the potential of BRD4-degradation molecules based on M1 and L1. The inspiration occurred from the work by Bradner et al., where dBET-1, a conjugate of JQ-1 and phthalimide (an E3 ligase recognition moiety), was developed as a PROTAC capable of inducing proteasome degradation of BRD4 in cells.<sup>40</sup> Thus, we attempted to generate a PROTAC molecule by fusing the C-terminus of M1 or L1 to a proteasome-targeting motif, PTM (Figure 4a). A tetrapeptide consisting of RRRG (which might also aid the cell penetration) was selected as a PTM since previous studies have shown that proteins are amenable to proteolysis when specific ligands are attached to this tetrapeptide.<sup>41,42</sup> We have designed the combination of M1 or L1 conjugated with the RRRG peptide linker; Consequently, four potential PROTACs, M1-PEG-PTM, L1-PEG-PTM, M1-GSGS-PTM, and L1-GSGS-PTM, were synthesized. A breast cancer cell line (MCF-7) was treated with 10  $\mu\text{M}$  of each molecule for 4 h and endogenous BRD4 levels were analyzed by immunoblot. Consequently, M1-PEG-PTM exhibited the best degradation activity, reducing the BRD4 level to approximately 50% compared with the untreated level (Figure 4b). L1-PEG-PTM also exhibited a modest but detectable activity. These activities were inhibited in the presence of proteasome inhibitor I, indicating that BRD4 was most likely degraded via proteasome pathways (Figure 4c,d). In contrast, the other two peptides with GSGS linkers did not show activity, suggesting that the peptide linker was not suitable, presumably due to an unfavorable negative impact on the membrane permeability of the molecule.

We then titrated the concentrations of M1-PEG-PTM from 1.25 to 10  $\mu\text{M}$  in a 4 h period. We observed a concentration-dependent degraon activity of M1-PEG-PTM, reducing the BRD4 level to 42% at 10  $\mu\text{M}$ , which was consistent with the earlier observation (Figure 4e).

### DISCUSSION AND CONCLUSIONS

In this work, we have designed <sup>CIMe</sup>BPy as the N-terminal building block of peptides and ribosomally expressed a macrocyclic peptide library closed between <sup>CIMe</sup>BPy and a downstream Cys residue. The design was based on an expectation that the BPy moiety could act as a hydrophobic linkage and, at the same time, their pyridine nitrogen could form internal hydrogen bonds located in the opposite strand of the peptide sequence upon macrocyclization. We supposed that these properties might beneficially contribute to the

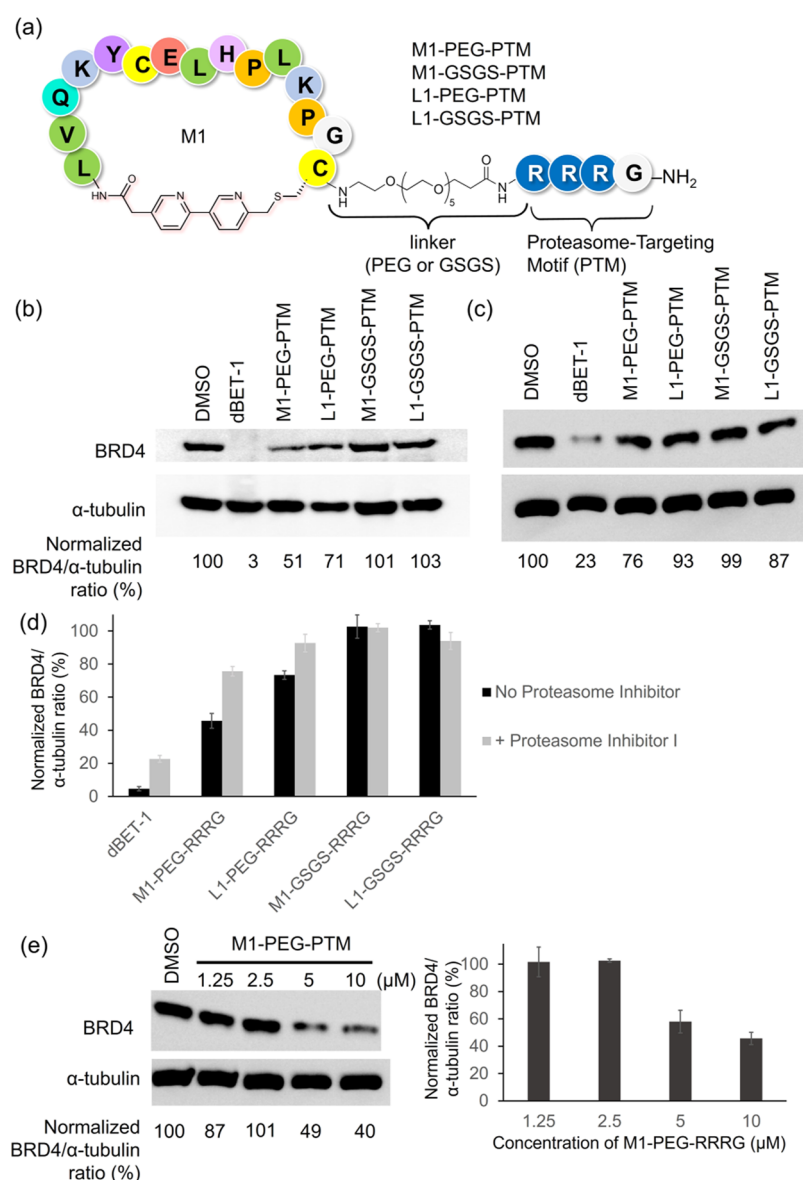


**Figure 4.** Proteolysis-targeting chimera (PROTAC) based on macrocycles and a proteasome-targeting motif (PTM). (a) Design of PROTAC peptides based on M1 and L1. A tetrapeptide motif, RRRG, was used as PTM that targets E3 ligase. Two different linkers, PEG (as shown in the figure) and GSGS, were added between M1 (or L1) and PTM. (b) Immunoblot for BRD4 and  $\alpha$ -tubulin after treatment of MCF-7 cells for 4 h with the indicated substances (final concentrations are 10  $\mu$ M for peptides and 1  $\mu$ M for dBET-1). (c) Immunoblot for BRD4 and  $\alpha$ -tubulin after treatment of MCF-7 cells for 4 h with the indicated substance (concentrations same as those in panel (b) and 1  $\mu$ M protease inhibitor I). (d) Histogram of BRD4 levels in panels (4b, c) (3 independent experiments respectively). The degradation was inhibited in the presence of protease inhibitor I ( $p < 0.005$  at the significance level of 0.05). (e) Immunoblot for BRD4 and  $\alpha$ -tubulin after treatment of MCF-7 cells for 4 h with 4 various concentrations (1.25–10  $\mu$ M) of M1-PEG5-PTM (three independent experiments, BRD4 levels were shown in the histogram).

membrane permeability of peptides, as demonstrated in our model peptide study (Figure 2).

The RaPID campaign in this study yielded only a single species of the peptide sequence enriched against BRD4<sup>49–460</sup>. However, in our past RaPID campaigns, we generally obtained multiple families of peptide sequences,<sup>43,44</sup> and therefore, this outcome was unusual. A probable explanation would be a loss of library diversity. This was mainly attributed to the poor initiation efficiency of <sup>CLM</sup>BPY-tRNA<sub>CAU</sub><sup>fMet</sup> in the FIT system, which resulted in a reduction of the overall expression of the peptide library, and this would lead to the reduction of library diversity. Indeed, qualitative evaluation of translated peptides using LC/MS also supported this possibility, where the expression level of <sup>CLM</sup>BPY-initiated model peptides was

about 10-fold lower than its ClAc-tyrosine-initiated analogue (Figure S4b). Thus, there is room to improve the initiation efficiency for the library construction in our future experiment.

In the present study, we demonstrated the enhancement of the cell membrane permeability of model peptides, BPY1/2 (Figure 2a), as well as selected peptides, M1, L1, and L1.7 (Figure 3a), conjugated to a chloroalkane tag by means of CAPA. Interestingly, neither peptide cyclization mode (macrocycle vs. lariat macrocycle) nor length (where L1.7 lacks the tail peptide, having less than half of the L1 size) in the latter macrocycles did not change their membrane permeability (Figure 3b). Thus, the BPY linkage seems to be a major determinant in enhancing the membrane permeability of

macrocycles despite the sequence composition, which also matters to a certain extent.

We synthesized BRD4-binding BPy macrocycles conjugated with RRRG-tetrapeptide as a PTM motif and tested if they exhibited PROTAC activity against BRD4. The best molecule developed in this study, M1-PEG-PTM, induced the degradation of BRD4 to the level of 50% at 10  $\mu\text{M}$ . However, the observed activity is limited compared with a commercially available PROTAC, dBET-1. This could be attributed to the insufficient permeability of macrocycles into not only cells but also the nucleus to reach BRD4. Another issue could be the peptidic PTM used in this study, which might not be proteolytically stable enough in cells. Since these shortcomings could also account for the limited degron activity, further optimization of the peptide–PTM conjugate is critical in enhancing the degron performance of the macrocycles.

In conclusion, our demonstration reported here has shown that the choice of a  $\text{C}^{\text{IMe}}$ BPy initiator to macrocyclize the peptide sequences with the BPy unit is able to contribute to an enhancement of their cell membrane permeability. Although the tertiary structure generated by the BPy is yet to be elucidated, we envision that such an approach by designing more extensive kinds of pyridyl-based linkages of macrocycles will lead us to even better membrane-permeable peptides. The power of RaPID display selection coupled with not only initiation reprogramming but also elongation reprogramming will allow us to further explore such a molecular space that we have not explored before.

## EXPERIMENTAL SECTION

### Materials

Chemical reagents used in synthesis were purchased from Tokyo Chemical Industries, Wako Pure Chemical Industries, Sigma-Aldrich (Merck) Japan, Nacalai Tesque, and Watanabe Chemical Industries and were used without further purification unless specified. All oligonucleotide primers were purchased from Eurofin Genomics (Japan) as 100 pmol/ $\mu\text{L}$  aqueous solutions after OPC purification. All other reagents were purchased from Thermo Fisher (Invitrogen), Bio-Rad, Cytiva, and Promega unless specified. The BRD4 (BD1 + BD2) TR-FRET assay kit was bought from BPS Bioscience (#32612). The detailed protocol for the chemical synthesis of small molecules and preparations of nucleic acids are provided in the (Supporting Information).

### In Vitro Translation of Peptides

To the amino acid-free in vitro translational system mixture (1.5  $\mu\text{L}$ , see the Supporting Information for details) were added an amino acid mixed solution (5 mM of 19 amino acids without Met, 0.25  $\mu\text{L}$ ) and template DNA encoding the peptide sequence MVYNTRSGWRWYTC(GS)<sub>3</sub> (0.4 mM, 0.25  $\mu\text{L}$ ), and then  $\text{C}^{\text{IMe}}$ B-Py-tRNA<sub>CAU</sub><sup>fMet</sup> (amount varied according to final concentrations shown in Figure S2b) or  $\text{C}^{\text{IAC}}$ Y-tRNA<sub>CAU</sub><sup>fMet</sup> (125 pmol) was added in 0.5  $\mu\text{L}$  of 1 mM NaOAc. The resultant 2.5  $\mu\text{L}$  of reaction solution was translated at 37 °C for 30 min and then applied to mass spectrometry. MALDI samples were desalted with SPE C-Tip (Nikkyo Technos) prior to detection. LC/MS samples were diluted with 47.5  $\mu\text{L}$  of 1% TFA solution and centrifuged at 13,000 rpm for 5 min before injection. 10  $\mu\text{L}$  of the resultant supernatant was used for LC/MS analysis with a linear gradient of buffer B from 5 to 80%.

### RaPID Selection of Peptides against BRD4 (Bromodomains 1 and 2)

The macrocyclic peptide library was translated at 37 °C for 30 min in the in vitro translation system described above. The reaction volume was 150  $\mu\text{L}$  for the 1st round of selection and 5  $\mu\text{L}$  for the other rounds. After the translation was finished, the reaction solution was

first incubated at room temperature for 5 min and then mixed with a 0.2 $\times$  volume of 500 mM EDTA (pH 8.0) and incubated at 37 °C for 12 min to disassemble ribosome and release mRNA-peptide conjugates. Reverse transcription was then carried out at 42 °C for 30 min, and the resultant cDNA–mRNA–peptide conjugates were applied to a desalting column (Sephadex G-25 resin in TBS-T buffer). The desalted sample was mixed with a 1 $\times$  translation volume of Dynabeads (His-tag) and incubated at 4 °C for 1 min for 3 times as preclearance, and the supernatant was mixed with a 1.2 $\times$  translation volume of Dynabeads (His-tag) and incubated at 4 °C for 30 min for 6 times as a negative selection (which was not applied in the 1st round of selection). The resultant supernatant was then mixed with a 0.2 $\times$  translation volume of His10-BRD4 (49–460)-immobilized Dynabeads (His-tag) and incubated at 4 °C for 30 min as a positive selection. After that, the beads from the negative selection and the positive selection were washed with 100  $\mu\text{L}$  of ice-cooled TBS-T buffer 3 times and then resuspended in 100  $\mu\text{L}$  of PCR premix solution and incubated at 95 °C for 5 min. The amount of recovered cDNA from the beads (negative and positive selections) was determined by real-time PCR using 1  $\mu\text{L}$  of the eluate, and the recovery rate was calculated according to the precleared samples. The recovered cDNA from the positive selection was amplified by PCR and then transcribed to give the peptide library for the next round of selection.

### Chemical Synthesis of Peptides

The peptides were chemically synthesized by standard Fmoc solid-phase peptide synthesis (SPPS) using a Biotage Syro Wave peptide synthesizer. The Rink Amide resin (54 mg, 25  $\mu\text{mol}$ ) was applied for each peptide. The deprotection of Fmoc was carried out at room temperature by incubating the resin with 40% piperidine/DMF for 3 min and 20% piperidine/DMF for 12 min. After deprotection, the resin was washed with DMF 5 times. Then, Fmoc-protected amino acid was coupled for 40 min at 30 °C by incubating the resin with a solution in DMF containing 0.2 M Fmoc-protected amino acid, 0.2 M HBTU, 0.2 M HOBt, and 0.1 M DIPEA. The coupling was repeated once, and the resin was washed with DMF 5 times and then deprotected for the next residue. The coupling of the PEG linker in PROTAC peptides was conducted for 1 h at room temperature twice in a solution of DMF containing a 0.15 M Fmoc-protected PEG linker, 0.2 M PyBOP, and 0.1 M DIPEA. The coupling of a bipyrindyl initiator (or biphenyl initiator) was conducted overnight at room temperature in a solution of DMF containing 0.15 M  $\text{C}^{\text{IMe}}$ BPy–COOH ( $\text{C}^{\text{BrMe}}$ BPh–COOH in the case of biphenyl-initiated peptides), 0.2 M PyBOP, and 0.3 M DIPEA. For tyrosine-initiated peptides, the *N*-chloroacetamide group was introduced by incubating the resin with 1 mL of 0.2 M chloroacetyl *N*-hydroxysuccinimide ester (ClAc-NHS) for 1 h at room temperature. After coupling the bipyrindyl initiator or introducing the *N*-chloroacetamide group, the Mmt protecting groups (Cys or Lys) were removed by incubating the resin with a solution of DCM containing 2% TFA and 2.5% TIS several times until the solution became colorless. Peptides that contain the selected peptide sequence ( $\text{C}^{\text{IMe}}$ BPy-LVQKYCELHPLKPGC) were then treated with 5% DIPEA in DMF overnight for the cyclization, and peptides used for CAPA were coupled with the chloroalkyl linker at their C-terminal Lys residues by incubating the resins with a solution of DMF containing a 0.15 M chloroalkyl linker,<sup>29</sup> 0.2 M PyBOP, and 0.1 M DIPEA overnight. The resins were washed with DMF and DCM, respectively, 3 times and completely dried, and the peptides were cleaved off by 2 mL of a peptide cleavage cocktail under rotation for 3 h and then concentrated in vacuo. The residues were mixed with diethyl ether, and the precipitated peptides were dried and then dissolved in 2 mL of DMSO. For peptides with single cysteine, 2 mL of water and 60  $\mu\text{L}$  of DIPEA were added and then rotated overnight for cyclization (60  $\mu\text{L}$  of TFA was added to neutralize DIPEA upon completion). Finally, the peptides were purified by reversed-phase HPLC (purities of all chemically synthesized peptides are over 90%, traced by UPLC), and their identities were confirmed by MALDI-TOF MS (Figure S4). Peptides that were used for biological assays were changed to their chloride by TFA-HCl exchange (the peptide

was dissolved in 10 mM HCl and 50% acetonitrile in water and the solution was lyophilized) 3 times before use.

### Evaluation of Binding Affinity by SPR

The binding affinities of the selected peptides (M1G and L1G) against BRD4 (bromodomains 1 and 2) were evaluated by SPR using a Biacore T200 instrument. Measurements were performed at 25 °C using the HBS-EP+ buffer containing 0.1% DMSO (w/w) for running buffer. Following standard immobilization protocols provided by the manufacturer, His10-BRD4 (49–460) was immobilized on a series S sensor chip (NTA) to a surface density of 1000–1200 response units (RUs). Sensorgrams were obtained by the single-cycle kinetics method by successive injection of five different concentrations of each peptide at a flow rate of 30  $\mu$ L/min. The resulting sensorgrams were analyzed by the standard 1:1 interaction model using Biacore evaluation software (Figure S5).

### Serum Stability Assay

A 10  $\mu$ M peptide (M1G, L1G, R9, and Tat) and 10  $\mu$ M internal standard peptide (H<sub>2</sub>N-PEG<sub>5</sub>-wstndwstnd-PEG<sub>5</sub>-CONH<sub>2</sub>) consisting of D-amino acids were incubated in human serum (Cosmo Bio) at 37 °C for up to 50 h. At each time point, 4.5  $\mu$ L of the mixture was sampled and mixed with 12  $\mu$ L of ethanol and cooled on ice for 5 min and then centrifuged at 13,000 rpm for 3 min. 10  $\mu$ L of the supernatant was mixed with 40  $\mu$ L of 1% TFA and centrifuged at 13,000 rpm for another 3 min. 2  $\mu$ L of the resultant supernatant was used for LC/MS analysis with a linear gradient of buffer B from 1 to 60%. The stability of the peptide was estimated by the relative intensity of the selected peptide to the internal standard peptide, which would not degrade under these experiment conditions.

### Evaluation of Membrane Permeability by CAPA

HEK293 (Mito-Halo overexpressed) cells were cultured in DMEM supplemented with 10% FBS and 1% penicillin/streptomycin and then transferred to collagen-I-coated 96-well plates with a population of 40,000 cells in each well. After grown for 24 h, the cells were incubated in the working medium (Opti-MEM supplemented with 5% FBS, 1% penicillin/streptomycin, and 1% DMSO) and chloroalkane-tagged peptides (peptide-CAs) at indicated concentrations (shown in Figures 2b, 3c, and S2, as well as blank samples) and cultured for another 4 or 24 h. The cells were washed with the working medium and then treated with a working medium supplemented with 50  $\mu$ M chloroalkane-tagged TAMRA (TAMRA-CA) and cultured for 15 min. The cells were washed with the working medium 3 times and then detached from the plates by trypsin digestion. The quantified fluorescence of the cells was measured by a Cytoflex flow cytometry at the wavelength of 564 nm and fitted with a sigmoidal curve using Prism software.

### In Vitro Degradation of PROTAC Peptides

MCF-7 cells were cultured in DMEM supplemented with 10% FBS and 1% penicillin/streptomycin and then transferred to 6-well plates. After the population of cells in each well reached 10<sup>6</sup>, the cells were treated with DMEM supplemented with 1% penicillin/streptomycin, 0.1% DMSO, and PROTAC peptides at indicated concentrations (shown in Figure 4b,c,e) and cultured for 4 h. The cells were detached from the plate by trypsin digestion, washed with 1 $\times$  PBS buffer several times, and then lysed using RIPA buffer supplemented with a protease inhibitor cocktail and 0.1% benzonase on ice for 30 min. The lysates were centrifuged at 15,000 rpm for 20 min at 4 °C, and the protein concentrations in the supernatants were determined using a BCA assay. The samples were separated with 7.5% SDS-PAGE gels and transferred to PVDF membranes using an iBlot 2 Dry Blotting System and then immunoblotted with an HRP-conjugated BRD4 antibody (abcam) and  $\alpha$ -tubulin antibody (MBL). The blots were imaged with an ECL detection reagent on a chemiluminescent imager, and the band intensities were analyzed by ImageJ software.

## ■ ASSOCIATED CONTENT

### Supporting Information

The Supporting Information is available free of charge at <https://pubs.acs.org/doi/10.1021/acsbiomedchemau.3c00027>.

Materials and methods in detail, additional data figures and tables, chemical structures, and characterization (PDF)

## ■ AUTHOR INFORMATION

### Corresponding Author

Hiroaki Suga – Department of Chemistry, Graduate School of Science, The University of Tokyo, Bunkyo-ku, Tokyo 113-0033, Japan; [orcid.org/0000-0002-5298-9186](https://orcid.org/0000-0002-5298-9186); Email: [hsuga@chem.s.u-tokyo.ac.jp](mailto:hsuga@chem.s.u-tokyo.ac.jp)

### Authors

Hongxue Chen – Department of Chemistry, Graduate School of Science, The University of Tokyo, Bunkyo-ku, Tokyo 113-0033, Japan

Takayuki Katoh – Department of Chemistry, Graduate School of Science, The University of Tokyo, Bunkyo-ku, Tokyo 113-0033, Japan; [orcid.org/0000-0001-6550-6203](https://orcid.org/0000-0001-6550-6203)

Complete contact information is available at: <https://pubs.acs.org/10.1021/acsbiomedchemau.3c00027>

### Author Contributions

H.S. designed the research program and supervised it. H.C. conducted the research and analyzed the data. H.S. and H.C. wrote and revised the manuscript, and T.K. supervised the experimental details and revised the manuscript.

### Funding

The Japan Society for the Promotion of Science (JSPS), KAKENHI, Specially Promoted Research (JP19K22243) to H.S.

### Notes

The authors declare no competing financial interest.

## ■ ACKNOWLEDGMENTS

We are grateful to Prof. Joshua Kritzer for sharing their expertise on CAPA.

## ■ REFERENCES

- (1) Vinogradov, A. A.; Yin, Y.; Suga, H. Macrocyclic peptides as drug candidates: recent progress and remaining challenges. *J. Am. Chem. Soc.* **2019**, *141*, 4167–4181.
- (2) Zorzi, A.; Deyle, K.; Heinis, C. Cyclic peptide therapeutics: past, present and future. *Curr. Opin. Chem. Biol.* **2017**, *38*, 24–29.
- (3) Huang, Y.; Wiedmann, M. M.; Suga, H. RNA display methods for the discovery of bioactive macrocycles. *Chem. Rev.* **2019**, *119*, 10360–10391.
- (4) Passioura, T.; Suga, H. Flexizymes, their evolutionary history and diverse utilities. *Top. Curr. Chem.* **2014**, *344*, 331–345.
- (5) Vinogradov, A. A.; Suga, H. Introduction to thiopeptides: biological activity, biosynthesis, and strategies for functional reprogramming. *Cell Chem. Biol.* **2020**, *27*, 1032–1051.
- (6) Katoh, T.; Suga, H. Engineering translation components improve incorporation of exotic amino acids. *Int. J. Mol. Sci.* **2019**, *20*, 522.
- (7) Katoh, T.; Iwane, Y.; Suga, H. tRNA engineering for manipulating genetic code. *RNA Biol.* **2018**, *15*, 453–460.

- (8) Vamiseti, G. B.; Saha, A.; Huang, Y. J.; Vanjari, R.; Mann, G.; Gutbrod, J.; Ayoub, N.; Suga, H.; Brik, A. Selective macrocyclic peptide modulators of Lys63-linked ubiquitin chains disrupt DNA damage repair. *Nat. Commun.* **2022**, *13*, No. 6174.
- (9) Haberman, V. A.; Fleming, S. R.; Leisner, T. M.; Puhl, A. C.; Feng, E.; Xie, L.; Chen, X.; Goto, Y.; Suga, H.; Parise, L. V.; Kireev, D.; Pearce, K. H.; Bowers, A. A. Discovery and development of cyclic peptide inhibitors of CIB1. *ACS Med. Chem. Lett.* **2021**, *12*, 1832–1839.
- (10) Kawamura, A.; Münzel, M.; Kojima, T.; Yapp, C.; Bhushan, B.; Goto, Y.; Tumber, A.; Katoh, T.; King, O. N.; Passioura, T.; Walport, L. J.; Hatch, S. B.; Madden, S.; Müller, S.; Brennan, P. E.; Chowdhury, R.; Hopkinson, R. J.; Suga, H.; Schofield, C. J. Highly selective inhibition of histone demethylases by de novo macrocyclic peptides. *Nat. Commun.* **2017**, *8*, No. 14773.
- (11) Hewitt, W. M.; Leung, S. S.; Pye, C. R.; Ponkey, A. R.; Bednarek, M.; Jacobson, M. P.; Lokey, R. S. Cell-permeable cyclic peptides from synthetic libraries inspired by natural products. *J. Am. Chem. Soc.* **2015**, *137*, 715–721.
- (12) Ahlback, C. L.; Lexa, K. W.; Bockus, A. T.; Chen, V.; Crews, P.; Jacobson, M. P.; Lokey, R. S. Beyond cyclosporine A: conformation-dependent passive membrane permeabilities of cyclic peptide natural products. *Future Med. Chem.* **2015**, *7*, 2121–2130.
- (13) Furukawa, A.; Townsend, C. E.; Schwochert, J.; Pye, C. R.; Bednarek, M. A.; Lokey, R. S. Passive membrane permeability in cyclic peptomer scaffolds is robust to extensive variation in side chain functionality and backbone geometry. *J. Med. Chem.* **2016**, *59*, 9503–9512.
- (14) Joliot, A.; Prochiantz, A. Transduction peptides: from technology to physiology. *Nat. Cell Biol.* **2004**, *6*, 189–196.
- (15) Doherty, G. J.; McMahon, H. T. Mechanisms of endocytosis. *Annu. Rev. Biochem.* **2009**, *78*, 857–902.
- (16) Lian, W.; Jiang, B.; Qian, Z.; Pei, D. Cell-permeable bicyclic peptide inhibitors against intracellular proteins. *J. Am. Chem. Soc.* **2014**, *136*, 9830–9833.
- (17) Jiang, B.; Pei, D. A Selective, Cell-permeable nonphosphorylated bicyclic peptidyl inhibitor against peptidyl-prolyl isomerase Pin1. *J. Med. Chem.* **2015**, *58*, 6306–6312.
- (18) Qian, Z.; Martyna, A.; Hard, R. L.; Wang, J.; Appiah-Kubi, G.; Coss, C.; Phelps, M. A.; Rossman, J. S.; Pei, D. Discovery and mechanism of highly efficient cyclic cell-penetrating peptides. *Biochemistry* **2016**, *55*, 2601–2612.
- (19) Choi, K. Y.; Chow, L. N.; Mookherjee, N. Cationic host defence peptides: multifaceted role in immune modulation and inflammation. *J. Innate Immun.* **2012**, *4*, 361–370.
- (20) Walensky, L. D.; Pitter, K.; Morash, J.; Oh, K. J.; Barbuto, S.; Fisher, J.; Smith, E.; Verdine, G. L.; Korsmeyer, S. J. A stapled BID BH3 helix directly binds and activates BAX. *Mol. Cell* **2006**, *24*, 199–210.
- (21) Muppidi, A.; Doi, K.; Ramil, C. P.; Wang, H. G.; Lin, Q. Synthesis of cell-permeable stapled BH3 peptide-based Mcl-1 inhibitors containing simple aryl and vinylaryl cross-linkers. *Tetrahedron* **2014**, *70*, 7740–7745.
- (22) Muppidi, A.; Zhang, H.; Curreli, F.; Li, N.; Debnath, A. K.; Lin, Q. Design of antiviral stapled peptides containing a biphenyl cross-linker. *Bioorg. Med. Chem. Lett.* **2014**, *24*, 1748–1751.
- (23) Bird, G. H.; Mazzola, E.; Opoku-Nsiah, K.; Lammert, M. A.; Godes, M.; Neuberger, D. S.; Walensky, L. D. Biophysical determinants for cellular uptake of hydrocarbon-stapled peptide helices. *Nat. Chem. Biol.* **2016**, *12*, 845–852.
- (24) Tian, Y.; Jiang, Y.; Li, J.; Wang, D.; Zhao, H.; Li, Z. Effect of stapling architecture on physicochemical properties and cell permeability of stapled alpha-helical peptides: a comparative study. *Chembiochem* **2017**, *18*, 2087–2093.
- (25) Muppidi, A.; Zou, H.; Yang, P. Y.; Chao, E.; Sherwood, L.; Nunez, V.; Woods, A. K.; Schultz, P. G.; Lin, Q.; Shen, W. Design of potent and proteolytically stable oxyntomodulin analogs. *ACS Chem. Biol.* **2016**, *11*, 324–328.
- (26) Muppidi, A.; Wang, Z.; Li, X.; Chen, J.; Lin, Q. Achieving cell penetration with distance-matching cysteine cross-linkers: a facile route to cell-permeable peptide dual inhibitors of Mdm2/Mdmx. *Chem. Commun.* **2011**, *47*, 9396–9398.
- (27) Chen, X.; Zaro, J. L.; Shen, W. C. Fusion protein linkers: property, design and functionality. *Adv Drug Delivery Rev.* **2013**, *65*, 1357–1369.
- (28) Arosio, P.; Owczarz, M.; Wu, H.; Butté, A.; Morbidelli, M. End-to-end self-assembly of RADA 16-I nanofibrils in aqueous solutions. *Biophys. J.* **2012**, *102*, 1617–1626.
- (29) Peraro, L.; Deprey, K. L.; Moser, M. K.; Zou, Z.; Ball, H. L.; Levine, B.; Kritzer, J. A. Cell Penetration profiling using the chloroalkane penetration assay. *J. Am. Chem. Soc.* **2018**, *140*, 11360–11369.
- (30) Tajima, K.; Katoh, T.; Suga, H. Drop-off-reinitiation triggered by EF-G-driven mistranslocation and its alleviation by EF-P. *Nucleic Acids Res.* **2022**, *50*, 2736–2753.
- (31) Katoh, T.; Suga, H. Drop-off-reinitiation at the amino termini of nascent peptides and its regulation by IF3, EF-G, and RRF. *RNA* **2023**, *29*, 663–674.
- (32) Zuber, J.; Shi, J.; Wang, E.; Rappaport, A. R.; Herrmann, H.; Sison, E. A.; Magoon, D.; Qi, J.; Blatt, K.; Wunderlich, M.; Taylor, M. J.; Johns, C.; Chicas, A.; Mulloy, J. C.; Kogan, S. C.; Brown, P.; Valent, P.; Bradner, J. E.; Lowe, S. W.; Vakoc, C. R. RNAi screen identifies BRD4 as a therapeutic target in acute myeloid leukaemia. *Nature* **2011**, *478*, 524–528.
- (33) Asangani, I. A.; Dommeti, V. L.; Wang, X.; Malik, R.; Cieslik, M.; Yang, R.; Escara-Wilke, J.; Wilder-Romans, K.; Dhanireddy, S.; Engelke, C.; Iyer, M. K.; Jing, X.; Wu, Y.-M.; Cao, X.; Qin, Z. S.; Wang, S.; Feng, F. Y.; Chinnaiyan, A. M. Therapeutic targeting of BET bromodomain proteins in castration-resistant prostate cancer. *Nature* **2014**, *510*, 278–282.
- (34) Shu, S.; Lin, C. Y.; He, H. H.; Witwicki, R. M.; Tabassum, D. P.; Roberts, J. M.; Janiszewska, M.; Jin Huh, S.; Liang, Y.; Ryan, J.; Doherty, E.; Mohammed, H.; Guo, H.; Stover, D. G.; Ekram, M. B.; Peluffo, G.; Brown, J.; D'Santos, C.; Krop, I. E.; Dillon, D.; McKeown, M.; Ott, C.; Qi, J.; Ni, M.; Rao, P. K.; Duarte, M.; Wu, S.-Y.; Chiang, C.-M.; Anders, L.; Young, R. A.; Winer, E. P.; Letai, A.; Barry, W. T.; Carroll, J. S.; Long, H. W.; Brown, M.; Shirley Liu, X.; Meyer, C. A.; Bradner, J. E.; Polyak, K. Response and resistance to BET bromodomain inhibitors in triple-negative breast cancer. *Nature* **2016**, *529*, 413–417.
- (35) Lu, L.; Chen, Z.; Lin, X.; Tian, L.; Su, Q.; An, P.; Li, W.; Wu, Y.; Du, J.; Shan, H.; Chiang, C. M.; Wang, H. Inhibition of BRD4 suppresses the malignancy of breast cancer cells via regulation of Snail. *Cell Death Differ.* **2020**, *27*, 255–268.
- (36) Filippakopoulos, P.; Knapp, S. Targeting bromodomains: epigenetic readers of lysine acetylation. *Nat. Rev. Drug Discovery* **2014**, *13*, 337–356.
- (37) Filippakopoulos, P.; Qi, J.; Picaud, S.; Shen, Y.; Smith, W. B.; Fedorov, O.; Morse, E. M.; Keates, T.; Hickman, T. T.; Felletar, I.; Philpott, M.; Munro, S.; McKeown, M. R.; Wang, Y.; Christie, A. L.; West, N.; Cameron, M. J.; Schwartz, B.; Heightman, T. D.; La Thangue, N.; French, C. A.; Wiest, O.; Kung, A. L.; Knapp, S.; Bradner, J. E. Selective inhibition of BET bromodomains. *Nature* **2010**, *468*, 1067–1073.
- (38) Patel, K.; Walport, L. J.; Walshe, J. L.; Solomon, P. D.; Low, J. K. K.; Tran, D. H.; Mouradian, K. S.; Silva, A. P. G.; Wilkinson-White, L.; Norman, A.; Franck, C.; Matthews, J. M.; Guss, J. M.; Payne, R. J.; Passioura, T.; Suga, H.; Mackay, J. P. Cyclic peptides can engage a single binding pocket through highly divergent modes. *Proc. Natl. Acad. Sci. U.S.A.* **2020**, *117*, 26728–26738.
- (39) Wernersson, S.; Bobby, R.; Flavell, L.; Milbradt, A. G.; Holdgate, G. A.; Embrey, K. J.; Akke, M. Bromodomain interactions with acetylated histone 4 peptides in the BRD4 tandem domain: effects on domain dynamics and internal flexibility. *Biochemistry* **2022**, *61*, 2303–2318.
- (40) Winter, G. E.; Buckley, D. L.; Paulk, J.; Roberts, J. M.; Souza, A.; Dhe-Paganon, S.; Bradner, J. E. Phthalimide conjugation as a



strategy for in vivo target protein degradation. *Science* **2015**, *348*, 1376–1381.

(41) Bonger, K. M.; Chen, L.-c.; Liu, C. W.; Wandless, T. J. Small-molecule displacement of a cryptic degron causes conditional protein degradation. *Nat. Chem. Biol.* **2011**, *7*, 531–537.

(42) Qu, J.; Ren, X.; Xue, F.; He, Y.; Zhang, R.; Zheng, Y.; Huang, H.; Wang, W.; Zhang, J. Specific knockdown of alpha-synuclein by peptide-directed proteasome degradation rescued its associated neurotoxicity. *Cell Chem. Biol.* **2020**, *27*, 751–762.e4.

(43) Katoh, T.; Sengoku, T.; Hirata, K.; Ogata, K.; Suga, H. Ribosomal synthesis and de novo discovery of bioactive foldamer peptides containing cyclic  $\beta$ -amino acids. *Nat. Chem.* **2020**, *12*, 1081–1088.

(44) Yin, Y.; Ochi, N.; Craven, T. W.; Baker, D.; Takigawa, N.; Suga, H. De novo carborane-containing macrocyclic peptides targeting human epidermal growth factor receptor. *J. Am. Chem. Soc.* **2019**, *141*, 19193–19197.